PHYSICAL REVIEW B VOLUME 52, NUMBER 20 15 NOVEMBER 1995-II

Scaling and dynamics of low-frequency hysteresis loops in ultrathin Co films on a Cu(001) surface

Q. Jiang, H.-N. Yang, and G.-C. Wang
Department of Physics, Applied Physics and Astronomy, Rensselaer Polytechnic Institute, Troy, New York 12180-3590
(Received 27 June 1995)

The hysteresis loops of epitaxially grown ultrathin Co films on a Cu(001) surface with magnetic anisotropy were measured *in situ* at room temperature under a periodic external field by the surface magneto-optical Kerr-effect technique. A dynamic phase transition occurs at high frequencies. At very low frequencies, Ω, a constant hysteresis loop area exists. We also observed power-law scaling of the loop area, $A \sim H_0^{\alpha}\Omega^{\beta}$, for $H_0 > 40$ Oe and $\Omega/2\pi < 90$ Hz, with exponents α and β each about $\frac{2}{3}$. The observations are consistent with a mean-field Ising model.

I. INTRODUCTION

Dynamic scaling behavior in nonequilibrium dissipative systems is a general phenomenon. It occurs in growing interfaces of submonolayers and thin films, diffusion-limited aggregation, the hysteresis loop in ferromagnetic systems, etc. These systems respond to a driving force and exhibit power-law scaling regardless of details in the system's free energy. The systems's response goes through a two-phase coexistence regime where the dynamics is slow and can be described by power laws. From the dynamic response and the values of scaling exponents one can classify the universality classes (depending on dimensionality and symmetry) from which mechanisms of growth, diffusion, or magnetization reversals can be learned. For the ferromagnetic system, the delay in magnetization reversal to the external driving field gives the hysteresis loop. The hysteresis loop area represents the energy loss in a magnetization-demagnetization cycle.

Qualitatively there are two kinds of dynamics magnetic models:[1,2] the continuous spin model and the Ising-like model. In a continuous spin system, magnetization reversal does not need to overcome an energy barrier. For such a system, recent analytical and numerical work[1-4] predicted that the area of the hysteresis loop scales with frequency Ω and field amplitude H_0 as $H_0^{\alpha}\Omega^{\beta}$. The exponents α and β are predicted[2] to have the same value, $\frac{1}{2}$. For Ising-like systems in which there exists an energy barrier for the order parameter (magnetization) to change sign, the dynamic scaling behavior has also been studied by many authors.[1,5-11] For example, in a mean-field Ising model,[7,11] an analytical solution exists for the scaling law with α and β each equal to $\frac{2}{3}$.

We believe that the ultrathin ferromagnetic films with uniaxial magnetization are good candidates for a real magnetic system that is consistent with an Ising-like model, where the spins have a continuous degree of freedom but the strong anisotropy introduces a large barrier for intermediate configurations. Our approach is to use ultrathin Co films grown on a Cu(001) surface, which has strong uniaxial magnetization with two ferromagnetic phases of opposite spin orientations. We used the surface magneto-optical Kerr-effect (SMOKE) technique[12,13] to measure the hysteresis loop at room temperature as a function of sinusoidal external magnetic field, $H(t)=H_0\sin(\Omega,t)$, with various field amplitudes H_0 and frequencies $f=\Omega/2\pi$ for 2- to 6-ML-thick Co films epitaxially grown *in situ* on a Cu(001) surface. A phase transition was observed at higher frequencies ($f \geq 350$ Hz) for a fixed ac current of 0.4 A. At very low frequencies ($f \leq 1$ Hz), we observed a constant area hysteresis loop. As the frequency increases, we found a scaling relationship: the loop area scales as $\sim\frac{2}{3}$ power law of H_0 and Ω. We also found that magnetization reversal and the hysteresis loop do not occur if H_0 is less then a threshold H_t. These observations are consistent with the mean-field Ising model.[7,11] Previously, we obtained a scaling relation in an Fe/Au(001) system[14] with $\alpha \sim \frac{2}{3}$ but $\beta \sim \frac{1}{3}$. It is believed that the frequency region where we extracted β is not low enough. Also, the magnetic anisotropy of Fe is not as strong as the Co system. The former may be close to a continuous spin system.

II. EXPERIMENTS

Our experiment was performed in an ultrahigh vacuum (UHV) chamber equipped with high-resolution low-energy electron diffraction[15] (HRLEED), SMOKE (Ref. 13), Auger electron spectroscopy, and a sputter ion gun. The sample was kept inside the UHV chamber during HRLEED and SMOKE measurements and there was no protective cover layer on the deposited Co film. The Co was evaporated from electron bombardment of a Co foil and the deposition rate can be changed by a factor of 10. The disklike Cu(001) substrate, with $\sim$1.9 cm diameter and $\sim$1.5 mm thickness, was characterized by HRLEED profile measurement. The LEED pattern shows a (1×1) pattern and the Cu surface has an average terrace width of $\sim$300 Å. The growth of submonolayer to 6-ML Co ultrathin films on a Cu(001) substrate at room temperature was monitored by HRLEED. In the submonolayer to $\sim$1.5-ML-thick regime, the HRLEED pattern shows a (1×1) unit mesh, which indicates that the Co film grows on the Cu(001) substrate with a face-centered-cubic structure.[16] When Co film is thicker than $\sim$1.5 ML, a $c(2\times2)$ pattern with weak half-order beams appears; this might

be induced from a small amount of C (Ref. 17) or from the Co and Cu intermixing at room temperature. This needs to be studied further.[18] The angular profiles of the (10) beam near the out-of-phase condition show characteristic changes of a near layer-by-layer growth, i.e., a decay in the peak intensity of the oscillation. The interface width extracted from the profile measurement[19] is about $0.5c$, where $c=1.76$ Å is the step height of Co. The deposition rate is 0.075 ML/min. An Auger scan shows dominant Co signals and less than 5% carbon contamination.

The magnetic field in the gap ($\sim$27 mm) of a C-shaped vanadium Permendur core was produced by passing a sinusoidal time-varying current through the Cu coil wound around the core. The external field is applied in the film plane and it is along the [100] (longitudinal) direction in the Co film. Note that the easy axis of the magnetization was orientated in the [110] direction.[20] The Kerr signal is collected after at least 10 cycles of initial magnetization and demagnetization loops to ensure that the Co film is well magnetized and the hysteresis loop is stable. The loop data are obtained by averaging over 40 cycles of scans. The phase difference between the effective magnetic field and the driving current in the coil was measured by comparing the output of a Hall sensor to the output of a bipolar power supply that provides the ac current in the coil. The result shows a lag of $\sim 5°-20°$ for 60–500 Hz. This phase delay of the output of the Hall sensor was used to correct the area of hysteresis loops by proper programming. The time-varying current or magnetizing field generates eddy currents in the core, which result in a counter field that reduces the magnitude of the applied field. The effective magnetic field was measured by two methods: the Hall sensor and a pickup core at the center of the gap (to replace the sample). The obtained normalized peak-to-peak voltage, which is proportional to the effective magnetic field, as a function of frequency at a fixed coil current, shows a drop in ($\sim$25%) the field amplitude at low frequencies (<80 Hz). This is our experimentally determined calibration curve $g(\Omega)$. The frequency-dependent effective magnetic field has been corrected by multiplying the calibration factor $g(\Omega)$ as used in the calculation of loop areas. We have measured the homogeneity of the field within the gap and perpendicular to the gap. The result shows a uniform field region of about $(0.5\text{ cm})^2$. The variation of the field amplitude in this region is less than 3%. The laser probing area in the Co film is less than $(0.5\text{ cm})^2$.

III. RESULTS AND MODEL ANALYSIS

A. Mean-field Ising model

To qualitatively understand the hysteresis process in an Ising-like system, one can start with a one-component time-dependent Landau-Ginzburg model where a double-well energy barrier is assumed so that the system can have two ferromagnetic states, described by the order parameter $\pm M_0$, with opposite signs. In cases where spatial fluctuations are suppressed, the magnetization M under an external sinusoidal field is described by mean-field dynamics,[1]

$$\frac{dM}{dt}=-(rM+uM^3)+H_0\sin(\Omega t)\ , \tag{1}$$

where the sum $rM+uM^3$ results from the double-well barrier and shows two ferromagnetic states with the order parameter $\pm M_0=\pm\sqrt{-r/u}$, where $r<0$ and $u>0$. From Eq. (1), one can show that the low-frequency behavior of the magnetization hysteresis is described by[7]

$$A(\text{hysteresis loop area})=\begin{cases} A_0+K[\Omega^2(H_0^2-H_{t0}^2)]^{1/3}, & H_0>H_t \\ 0, & H_0<H_t\ , \end{cases} \tag{2}$$

where $H_{t0}=\sqrt{-4r^3/27u}$, $A_0\sim 4M_0H_{t0}$, and K is a constant. H_t is equivalent to the coercivity of the magnetization and $H_t-H_{t0}\propto[\Omega^2(H_0^2-H_{t0}^2)]^{1/3}$.

The hysteresis loop characterized by Eq. (2) reveals three important properties for a mean-field Ising-like system. First of all, there exists a threshold field H_t as a result of the double-well barrier. If $H_0<H_t$, the field strength is not high enough to overcome the barrier for magnetization reversals so that no hysteresis loop exists, i.e., $A=0$. When the field amplitude H_0 increases from $H_0<H_t$ to $H_0>H_t$, the average order parameter over a cycle, $\langle M(t)\rangle$, jumps from a nonzero constant, $\langle M(t)\rangle\approx\pm M_0$ with $A=0$, to $\langle M(t)\rangle=0$ with $A>0$. The second characteristic indicated by Eq. (2) is that as $\Omega\to 0$, the magnetization process shows a constant loop area $A_0\sim 4M_0H_{t0}$. This comes from adiabatic magnetization reveals of magnetic domains between $M\approx M_0$ and $M\approx -M_0$, which can only occur at $H=\pm H_{t0}=\pm\sqrt{-4r^3/27u}$, in the presence of a double-well potential, with spatial fluctuations being negligible in the time scale considered. The third important features is the dynamic effect when $\Omega>0$. As the frequency increases, the magnetization cannot quickly respond to the rapidly varying field. Such a delay increases the loop area, as indicated by the term $K[\Omega^2(H_0^2-H_{t0}^2)]^{1/3}$, shown in Eq. (2). The dynamic hysteresis behavior thus manifests itself in the scaling relation[7,11] $A\sim H_0^{\alpha}\Omega^{\beta}$, with $\alpha=\beta=\frac{2}{3}$, for $H_0\gg H_{t0}$. It can be demonstrated[11] that various other mean-field Ising models as well as the demagnetization model[21] exhibit the three similar dynamic properties. We shall show later that these three important characteristics have been realized in the Co/Cu(100) system.

B. Dynamic phase transition at high frequencies

In the following we show data taken at room temperature from $\sim$3-ML Co films. Similar results are also obtained from 2-, 4-, 5-, and 6-ML films, but the data will not be shown here. Figure 1 shows the hysteresis loop area as a function of frequency with a current fixed at 0.4 A, which generates a frequency-dependent equivalent field amplitude $H_0=73.1$ Oe at the middle of the frequency range studied. The area increases with frequency first, reaches a maximum at $f\sim 85$ Hz, and then decreases at high frequencies. If Ω increases to the high-frequency region ($f\sim 350$ Hz), the loop area becomes distorted and

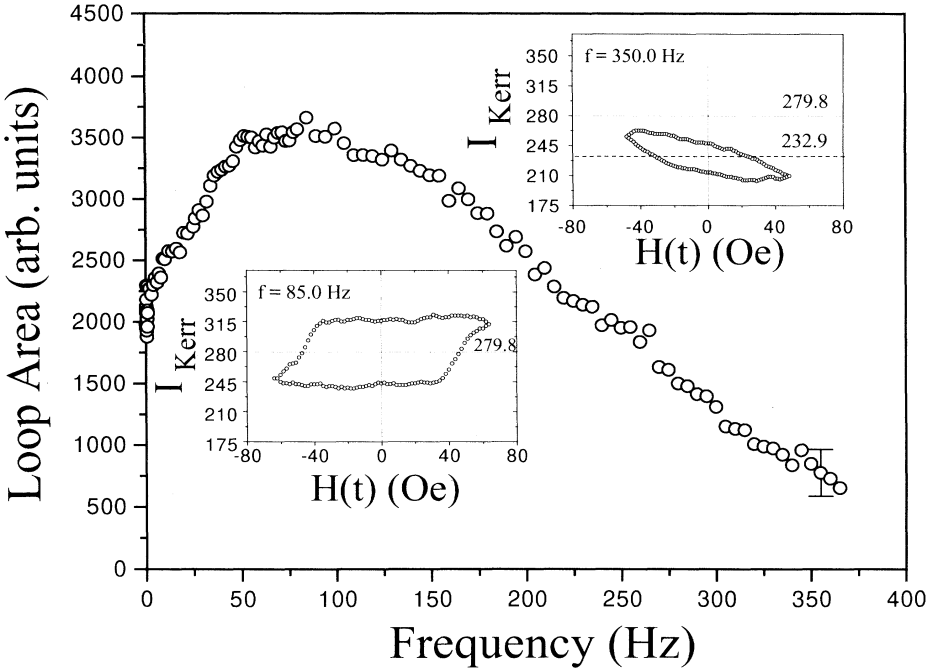

FIG. 1. The hysteresis loop area as a function of frequency is plotted at a fixed ac current of 0.4 A. The direction of the magnetic field is applied parallel to the film plane. The ac current generates not only a primary applied magnetic field $H(t)=H_0\sin(\Omega t)$ but also a counter eddy current that reduces the applied magnetic field. The net effective magnetic-field magnitude H_0 thus varies from 83 to 48 Oe as the frequency increases from near zero to ~350 Hz. The two loops shown in the insets were measured at 85 and 350 Hz, respectively.

the average magnetization $\langle M(t)\rangle$ over a cycle is shifted away from the zero magnetization line, as seen from the inset at the upper right-hand corner in Fig. 1. This means that there is no inversion symmetry in the hysteresis loop and indicates a dynamic phase transition predicted by Rao, Krishnamurthy, and Pandit.[1] It can be understood that if the frequency is too fast and the spin reversals in magnetic domains take a long time compared with the switching field period, the magnetic domains just cannot respond in time and they stay in the initial magnetic state.

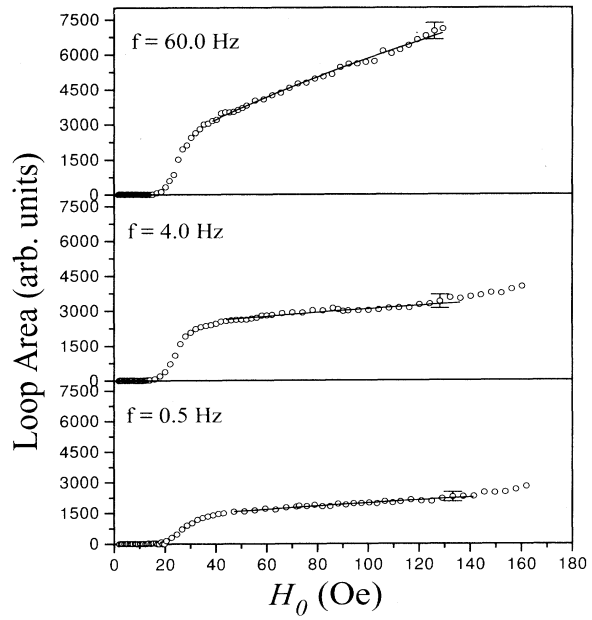

FIG. 2. The hysteresis loop area as a function of magnetic-field amplitude H_0 for several fixed frequencies. The solid curves are fits using the form $A=A_0+C(H_0^2-H_{t0}^2)^{\alpha/2}$, where A_0, C, H_{t0}, and α are adjustable parameters. The fit starts at $H_0>45$ Oe and the best fits give $\alpha=0.67\pm0.01$ and $H_{t0}=20.0\pm4.0$ Oe.

C. Threshold fields at low frequencies

The phase transition shown above exhibits the dynamic aspect of a ferromagnetic system at very high frequencies.[1] However, interesting phenomena were also shown in the lower-frequency regime, where the dynamic behavior predicted by Eq. (2) can be readily tested. Figure 2 is a plot of the loop area as a function of field amplitude H_0 for several fixed low frequencies. It is shown that below 20 Oe, the loop area is almost zero. As the field increases beyond 20 Oe, the area increases dramatically and slows down around 40 Oe. This clearly indicates that the hysteresis loops can only exist after a certain threshold field region H_t: 20–40 Oe. This is consistent with Eq. (2). Furthermore, we show in Fig. 3 the average magnetization over a cycle, $\langle M(t)\rangle$, as a function of the field amplitude H_0. When H_0 increases from $H_0<20$ to $H_0>40$ Oe, in addition to the rapid increases of the loop area shown in Fig. 2, $\langle M(t)\rangle$ jumps from a negative constant to zero, as shown in Fig. 3. The dramatic changes in both $\langle M(t)\rangle$ and A can be seen more clearly from the plot of $M(t)$ vs $H(t)$, shown as the inset in Fig. 3. At $H_0<H_t$, as shown in the left panel of the inset, the plot is a constant line. This implies that the loop area is zero and the system stays in the ferromagnetic state with a negative magnetization, $\langle M(t)\rangle=M(t)\approx-M_0$. Note that by reversing the direction of initial magnetization, we can also observe a similar behavior (not shown) for the positive magnetization state with

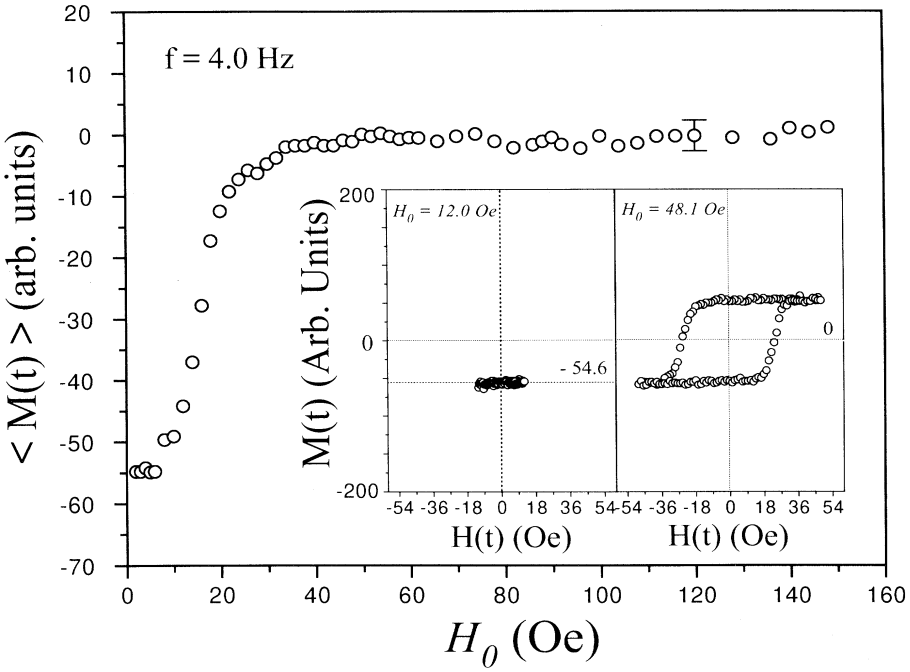

FIG. 3. The average magnetization over a cycle $\langle M(t)\rangle$ is plotted against the field amplitude H_0. The inset shows the plots of $M(t)$ vs $H(t)$ for two different fields: $H_0 < H_t$ (left panel) and $H_0 > H_t$ (right panel). Note that these curves are displayed in a coordinate system with the origin chosen at $M = H = 0$, i.e., the center of the hysteresis loop.

$\langle M(t)\rangle = M(t) \approx M_0$. However, when $H_0 > H_t$, the hysteresis loop develops as shown in the right panel of the inset, where the value of the saturated magnetization is exactly equal to M_0, the constant magnetization for $H_0 < H_t$ shown in the left panel. This indicates that, for $H_0 > H_t$, the magnetic domains are able to make reversals between two ferromagnetic states with order parameters of $-M_0$ and M_0. It leads to $\langle M(t)\rangle = 0$, i.e., the diminishing of the average order parameter $\langle M(t)\rangle$. The fact that the rise in both $\langle M(t)\rangle$ and A after the threshold is gradual and not sharp may be due to a distribution of domain sizes in the Co/Cu(100) film, provided domains have different thresholds.

D. Constant loop area at very low frequencies

The above observation confirms the existence of the threshold field H_t, which is consistent with the first characteristic contained in Eq. (2) for a mean-field Ising-

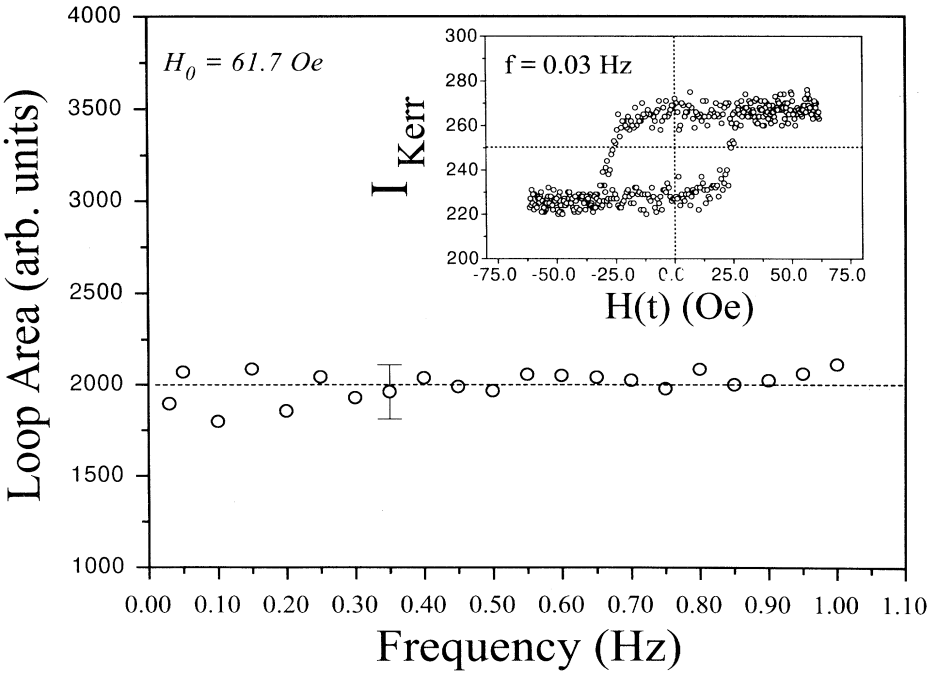

FIG. 4. The loop area as a function of frequency in the very-low-frequency regime, 0.03–1.00 Hz, with $H_0 = 62.1$ Oe. The inset shows a hysteresis loop measured at $f \sim 0.03$ Hz.

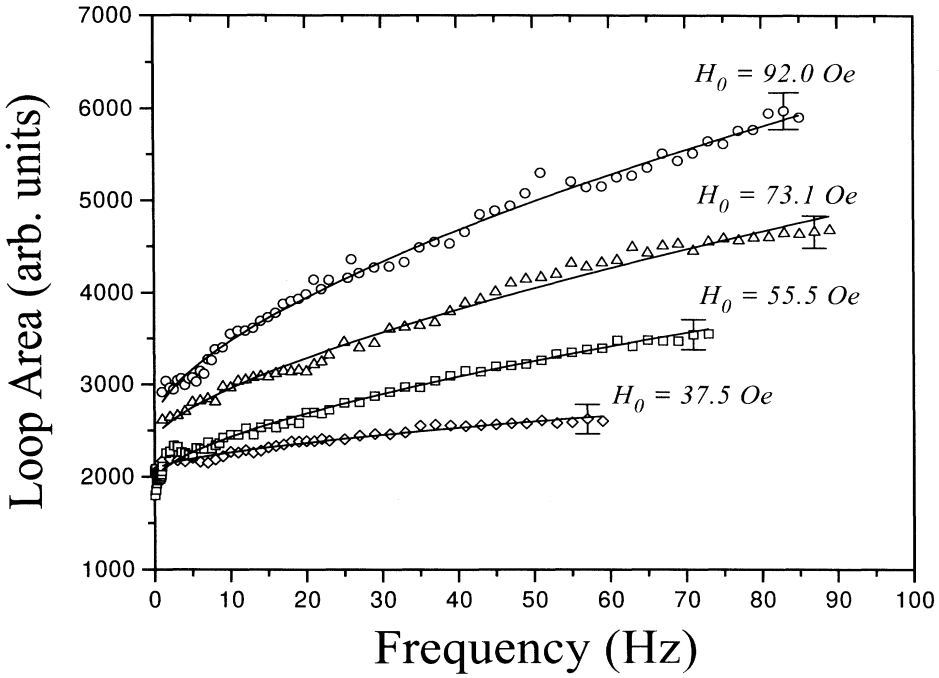

FIG. 5. The frequency-dependent hysteresis loop area at various fixed ac currents. The corresponding effective-field amplitude H_0 at mid-frequency is noted near each curve. Note that $\Omega=2\pi f$. The solid curves are fits using the form given by Eq. (2), where the field amplitude H_0 has been corrected by multiplying a frequency-dependent calibration factor $g(\Omega)$ due to the eddy current effect. The best fits give the exponent $\beta=0.66\pm0.03$.

like model. Furthermore, we can show that in the very-low-frequency regime 0.03–1.00 Hz, the hysteresis loops have a constant area for $H_0 > H_t$, as seen in Fig. 4. This behavior is consistent with the second feature in a mean-field Ising model, where the adiabatic magnetization has a constant hysteresis loop in the presence of a double-well behavior. Such a behavior is in contrast to the continuous spin systems where the loop area can go to zero as $\Omega \rightarrow 0$.[1,2]

E. Dynamic scaling at low frequencies and at low fields

To verify the Ω-dependent scaling law shown in Eq. (2), we plot in Fig. 5 the hysteresis area as a function of frequency at various fixed external fields H_0, all greater than H_t. Once the frequency increases beyond 1 Hz, the loop area increases. The higher the external field, the larger the area. The frequency-dependent areas can be fitted well by the solid curves that are described by Eq. (2) for $H > H_t$ with a constant A_0. Note that the field amplitude H_0 in Eq. (2) has to be corrected by the frequency-dependent eddy current effect. This is done by multiplying H_0 by a frequency-dependent calibration factor, $g(\Omega)$, which is an experimentally determined calibration curve. All fits show power-law dependence with an exponent $\beta=0.66\pm0.03$, which agrees with the dynamic scaling behavior shown in Eq. (2).

We can further examine the H_0-dependent scaling law. As shown in Fig. 2, beyond 40 Oe, (i.e., $H_0 > H_t$) the change of the area with H_0 can be fitted by Eq. (2) shown as solid curves. All the fits show that the data scales with H_0 as a power law with an exponent $\alpha=0.67\pm0.01$. Note that the slopes associated with the rise in area is frequency dependent. This is because the area also scales as a function of frequency at a fixed field amplitude, as shown in Fig. 5. From Figs. 2 and 5, we conclude that the dynamic scaling relation, $A \sim H_0^{\alpha}\Omega^{\beta}$, with $\alpha \approx \beta \approx \frac{2}{3}$, does exist in the Co/Cu(100) system, which is consistent with the dynamic characteristic indicated by Eq. (2). Notice that for ~3-ML film beyond the scaling region ($40 < H_0 < 120$ Oe), there seems to exist another region ($H_0 > 120$ Oe) where the area increases much faster. We speculate that a change of domain switching mechanism may be involved. Further study using a combination of real-time magnetic imaging techniques and hysteresis loops may help in understanding this change.

IV. DISCUSSION

To describe the dynamics in magnetic hysteresis realistically, many factors such as the magnetic anisotropy, nucleation barrier for magnetization to start (nucleation center, domain rotations, domain wall movements), and thermal fluctuation (random noise), etc., need to be considered. The dynamic phase transition is related to the relaxation time scale and potential barrier for magnetization reversal. The scaling relation provides the mechanism of magnetization reversal. Various ultrathin ferromagnetic films with different degrees of magnetic anisotropy being studied by many groups can be used as a testing ground for different universality classes by measuring the field amplitude and frequency-dependent hysteresis loops. Other experiments such as effects of temperature, thickness, and symmetry on dynamic phase transition and scaling should be of interest.

ACKNOWLEDGMENTS

This work was supported by ONR. We deeply appreciated K. Liang for the loan of the Cu(001) crystal. We also acknowledge A. Zangwill, M. Rao, R. Desai, A. Somoza, P. B. Thomas, and D. Dhar for their stimulating communications.

[1]M. Rao, H. R. Krishnamurthy, and R. Pandit, Phys. Rev. B **42**, 856 (1990); J. Phys. Condens. Matter **1**, 9061 (1991); M. Rao, Phys. Rev. Lett. **68**, 1437 (1992).

[2]D. Dhar and P. B. Thomas, J. Phys. A **25**, 4967 (1992); Europhys. Lett. **21**, 965 (1993); P. B. Thomas and D. Dhar, J. Phys. A **26**, 3973 (1993).

[3]M. Rao and R. Pandit, Phys. Rev. B **43**, 3373 (1990).

[4]A. M. Somoza and R. C. Desai, Phys. Rev. Lett. **70**, 3279 (1993).

[5]G. S. Agarwal and S. R. Shenoy, Phys. Rev. A **23**, 2719 (1981); **29**, 1315 (1984).

[6]T. Tomé and M. J. Oliveira, Phys. Rev. A **41**, 4251 (1990).

[7]Peter Jung, G. Gray, R. Roy, and P. Mandel, Phys. Rev. Lett. **65**, 1873 (1990); **68**, 1437 (1992).

[8]M. Acharyya, B. K. Chakrabarti, and A. K. Sen, Physica **A186**, 231 (1992); M. Acharyya and B. K. Chakrabarti, in *Annual Reviews of Computational Physics,* edited by D. Stauffer (World Scientific, Singapore, 1994), Vol. 1, p. 107; M. Acharyya and B. K. Chakrabarti, Physica A **192**, 471 (1993).

[9]W. S. Lo and R. A. Pelcovits, Phys. Rev. A **42**, 7471 (1990).

[10]S. Sengupta, Y. Marathe, and J. S. Puri, Phys. Rev. B **45**, 7828 (1992).

[11]C. N. Luse and A. Zangwill, Phys. Rev. E **50**, 224 (1994); (unpublished).

[12]E. R. Moog and S. D. Bader, Superlatt. Microstruct. **1**, 543 (1985).

[13]J.-P. Qian and G.-C. Wang, J. Vac. Sci. Technol. A **8**, 4117 (1990).

[14]Y.-L. He and G.-C. Wang, Phys. Rev. Lett. **70**, 2336 (1993); Y.-L. He, Y.-F. Liew, and G.-C. Wang, J. Appl. Phys. **75**, 5580 (1994).

[15]U. Scheithauer, G. Meyer, and M. Henzler, Surf. Sci. **178**, 441 (1986); J.-K. Zuo, R. A. Harper, and G.-C. Wang, Appl. Phys. Lett. **51**, 250 (1987).

[16]E. Navas, P. Schuster, C. M. Schneider, J. Kirschner, A. Cebollada, C. Ocal, R. Miranda, J. Cerdá, and P. de Andrés, J. Magn. Magn. Mater. **121**, 65 (1993); O. Heckmann, H. Magnan, P. le Fevre, D. Chandesris, and J. J. Rehr, Surf. Sci. **312**, 62 (1994).

[17]R. Miranda, D. Chandesris, and J. J. Lecante, Surf. Sci. **130**, 269 (1983); A. Clarke, G. Jennings, R. F. Willis, P. J. Rous, and J. B. Pendry, *ibid.* **187**, 327 (1987).

[18]Q. Jiang, H.-N. Yang, and G.-C. Wang (unpublished).

[19]H.-N. Yang, T.-M. Lu, and G.-C. Wang, *Diffraction From Rough Surfaces and Dynamic Growth Fronts* (World Scientific, Singapore, 1993).

[20]M. Kowalewski, C. M. Schneider, and B. Heinrich, Phys. Rev. B **47**, 8748 (1993).

[21]D. K. Lottis, R. M. White, and E. D. Dahlberg, Phys. Rev. Lett. **67**, 362 (1991).